2024 10th IEEE RAS/EMBS International Conference for
Biomedical Robotics and Biomechatronics (BioRob)
1-4 September 2024. Heidelberg, Germany

Augmented-Reality based digital twin to control an MR safe robot for breast biopsy: A benchmark study

Lennard Marx[1], Vincent Groenhuis[1], Stefano Stramigioli[1] and Kenan Niu[1]

***Abstract*— Magnetic resonance (MR) guided breast biopsies can be demanding and time-consuming procedures. Inaccurate needle insertion can yield false negatives, potentially leading to inaccurate diagnoses with severe consequences. Incorporating robots into these procedures has the potential to improve accuracy, alleviate patient strain, and reduce the time and cost of this procedure. A control interface is essential for surgeons to maintain control and make necessary adjustments. In this study, an augmented reality (AR)-based control method for surgeons is proposed by offering a new means of interacting with robots with enhanced intuition. A virtual surrogate of the MR safe robot in the AR scene was developed, which represents the digital embodiment of the actual robot in the physical world. Users can interact with the virtual surrogate robot to control the actual robot that is positioned in the MR bore while observing the 3D reconstruction of the clinical environment. Two AR-based interactive approaches (gesture-based control and auto-targeting) were developed and compared with joystick control. A pseudo-randomized study including ten subjects was conducted. Both gesture-based (2.24 mm) and auto-targeting (2.55 mm) control methods showed higher median accuracy than the joysticks (3.20 mm). This AR-based digital surrogate robot demonstrated the capabilities of coupling kinematics and motions of the physical MR safe robot for tasks in needle positioning and injection. It shows great potential to facilitate the clinical applications of MR safe robots in the future, beyond the MR-guided breast biopsy.**

I. INTRODUCTION

Breast cancer accounts for nearly one-third of cancer cases in women worldwide [1]. Given the rising prevalence and mortality rate of breast cancer, early diagnosis becomes increasingly important. The primary methods for the diagnosis of breast cancer are mammography and ultrasound. However, in cases involving a high risk of breast cancer, such as a high familial predisposition, mammography, even combined with ultrasound, may still prove insufficient for early detection [2]. The utilization of magnetic resonance imaging (MRI) has the potential to significantly enhance diagnostic sensitivity and enable earlier detection [2].

However, the MRI-guided breast biopsy procedure can be time-consuming and physically intensive for patients and clinicians [3]. To ensure precise needle placement during the biopsy, multiple MRI scans need to be conducted. In between these scans, the biopsy needle has to be re-positioned and oriented several times to reach the optimal pose. MR safe robots, exemplified by the Sunram7 (Figure 1, right), have the capacity to streamline this process by facilitating remote adjustments from a control room [4]. Augmented reality (AR) technology can be employed to visualize MRI images as three-dimensional (3D) objects through head-mounted displays (HMD) and facilitate intuitive path planning via projecting 3D Holographs of segmented anatomical structures [5]. Concurrently, AR can be used to interact with robots using gestures, voice commands, and holographic interfaces for intra-operative surgical procedures, like pedicle screw placement [6], [7]. An AR interface for teleoperating and potentially automating MR safe robots like the Sunram7 could significantly simplify the breast biopsy procedure, making it less of a burden for patients and more intuitive for surgeons (Figure 1). Moreover, it could reduce the duration and, consequently, the cost of the procedure. This, in turn, could enable MRI as a cost-effective diagnostic method, potentially increasing its utilization for early-stage diagnosis [8].

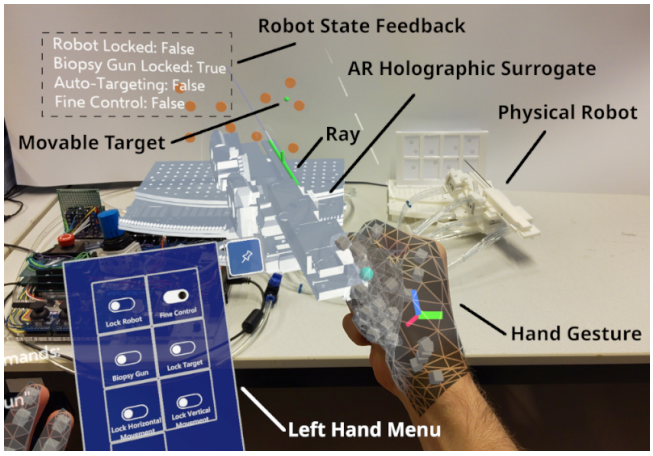

Fig. 1: The AR-based digital twin to control the Sumram7 robot (center left), and the physical robot (rightmost). The green dot indicates the movable target used in the auto-targeting mode. The left-hand menu is the graphic user interface (GUI) to toggle different functionalities.

State-of-the-art

At this point in time, augmented reality is predominantly used for visualization purposes and facilitating human-robot collaboration in various applications [6]. More importantly, there exists limited research on AR-based robot control in medical applications. For instance, Lin et al. developed a teleoperated robot for endoluminal interventions, which is controlled through gestures using an HMD (Figure 2a) [9]. A hologram of the trachea and the endoscope is presented

[1]Robotics and Mechatronics, University of Twente, Enschede, AE, The Netherlands l.marx@utwente.nl (L.M.), v.groenhuis@utwente.nl (V.G.), s.stramigioli@utwente.nl (S.S.), k.niu@utwente.nl (K.N.)

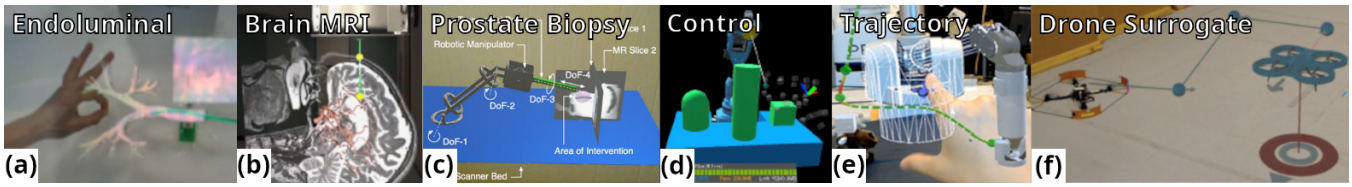

Fig. 2: Various AR-based interactive applications exerted from the state-of-the-art referenced here (Sec. I). (a): Lin et al. [9], (b): Morales Mojica et al. [10], (c): Velazco-Garcia et al. [11], (d): Xue et al. [12], (e): Quintero et al. [14], (f): Walker et al. [15].

in front of the user, allowing the user to manipulate the endoscope's position within the trachea through hand gestures. Similarly, Morales Mojica et al. used AR for image-guided control of interventional manipulators [10]. They visualized MRI images as holograms in front of the user, offering the ability to manipulate and display specific slices of the MRI scan. The AR interface was simultaneously used to control the manipulator, as well as to regulate the incision depth. This was done by defining a target point in a 2D plane and an incision point in the same plane, direct control of the robot was not possible. In a related study, Velazco-Garcia et al. conducted a comparative analysis of different input methods for planning MR-guided prostate biopsies [11]. They evaluated a holographic interface, comparing it with Gamepad and Mouse/Keyboard input methods. In this setup, the robot, along with the organs and lesions, were rendered as meshes in front of the user, enabling visualization of the robot's workspace. Notably, Velazco-Garcia et al. concluded that the AR input method yielded the least favourable results [11]. The sensitivity of the interactions with the holograms made it challenging to make precise adjustments along one dimension without inadvertently affecting another, ultimately deeming this method impractical.

While this paper primarily centres on the medical application of AR-based robot control, it is essential to provide a comprehensive overview of the state-of-the-art focusing on AR for robot control, including non-medical applications. Xue et al. introduced an AR-based robot control interface that allows users to manipulate the virtual end-effector to a desired position (Figure 2d) [12]. The inverse kinematics (IK) are resolved by the FABRIK method [13]. Additionally, they implemented collision detection to ensure a safe interaction with the environment. Quintero et al. programmed robots by defining trajectories within an AR environment [14]. These trajectories could be established by placing AR waypoints in 3D space, automatically generating a corresponding trajectory. Moreover, they introduced the capability to simulate tasks using a virtual surrogate before executing them with the physical robot. Issues were reported concerning the stability of hologram locations when operators moved while wearing the HMD. Walker et al. employed two distinct AR-based control methods to manage a drone via a holographic surrogate: real-time proportional–integral–derivative (PID) control and waypoint control [15]. Operators could either directly move the virtual surrogate, causing the drone to follow, or lock the drone's position and create waypoints by manipulating the virtual surrogate.

This paper aims to present an AR-based approach for intuitive interaction and teleoperation of an MR safe robot. The proposed method employs a head-mounted display (HMD) to showcase a holographic representation of the robot, referred to as the surrogate. This surrogate robot is digitally twinned with its physical counterpart, ensuring identical robotic executions. It allows the operator gain immersive control over the holographic surrogate outside the MRI room while enabling precise and coupled operations of the physical robot inside the MRI room. Inherent challenges in AR-based control were addressed, including the high sensitivity of the hologram, which may affect targeting accuracy. The proposed method holds the potential for a wide range of medical robot applications requiring teleoperation.

II. METHODS

A. Overview of the Framework

Figure 3 illustrates the system overview of the different technical components involved. The process begins with an MRI scan of the patient which is send to a computer and subsequently the Hololens2 HMD to generate the virtual scene. A zero position of the physical robot is assumed to align its joint space to the surrogate. In the control room, the operator wears the Hololens 2 HMD, which displays the holographic scene of the patient's MRI scan and virtual surrogate robot. By gesture inputs, the operator can control the surrogate robot by changing the desired position of the end-effector of the surrogate robot. This input is utilized to compute desired joint positions through IK and control the robot's dynamics via a controller. The operator receives instant visual feedback from the holographic scene to make necessary adjustments. Subsequently, the HMD simultaneously transmits the intended joint positions, either via a computer or directly to the robot's microcontroller, using WIFI connection. Finally, the robot executes the commands in the MRI room.

B. Sunram7 robot configuration

The physical robot in this paper is the Sunram7, shown in Figure 4. It's a five-degree-of-freedom MR safe robot designed for breast biopsy procedures [4]. To ensure compatibility with MRI environment, the robot was manufactured by 3D-printed plastic components. The Sunram7 utilizes pneumatic stepper motors for its actuation, which are also manufactured using rapid prototyping techniques [16]. Its

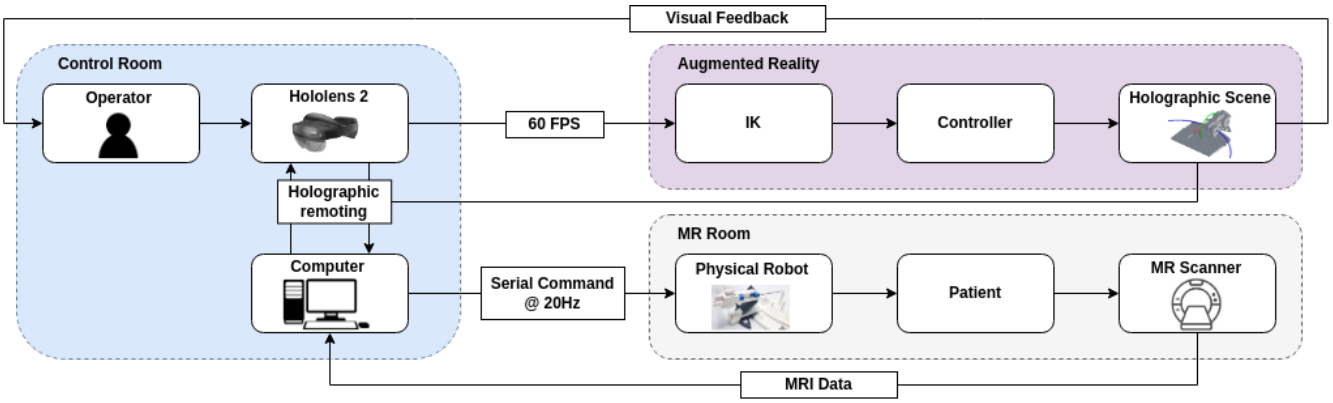

Fig. 3: The schematic overview of technical components and their connections in the AR-based robot control system.

(a) The Sunram7 robot.

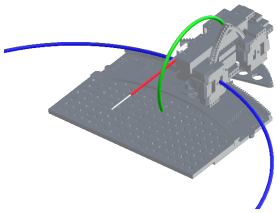

(b) The virtual surrogate.

Fig. 4: The physical robot (Sunram7) and its virtual surrogate. The blue and green circles on the surrogate represent the primary motion directions. The ray representing the desired pose is here depicted in red.

five degrees of freedom consist of four revolute joints and one prismatic joint. Specifically, two revolute joints facilitate horizontal movements of the robot, while the other two enable vertical motion. The prismatic joint controls the movement of the end-effector, being responsible for guiding the biopsy needle along its designated trajectory.

C. AR-based robotic control

For software development, the Unity game engine (Unity Technologies, San Francisco, U.S.) was employed in conjunction with the Mixed-Reality-Toolkit 2 (MRTK2) (Microsoft, Redmond, Washington, U.S.). The MRTK2 is an open-source software development kit (SDK) designed for creating mixed reality (MR) applications. The application was deployed on the Hololens 2 MR and AR HMD (Microsoft, Redmond, Washington, U.S.).

To generate the holographic representation of the robot, the same CAD (computer-aided design) files used for 3D printing the Sunram7 were imported into Unity and configured to replicate the robot's physical structure. A custom C# script was developed to solve the IK, allowing the robot's end-effector to align itself with a designated ray defining the desired position and orientation (Figure 4b). Due to the robot's design, the IK problem can be solved in two dimensions independently. Figure 4b illustrates the two main circles (blue circle for horizontal, green circle for vertical) on which the robot moves. In each dimension, two angles, denoted as θ_1 and θ_2, need to be calculated. This is achieved by first determining the intersection point of the ray with the circle and then deriving the angle offset of that point from the baseline (Figure 5). First, the perpendicular distance from the ray to the center of the circle is calculated to verify if it is smaller than the circle's radius. If it is not, no intersection can be found, as the ray is outside the robot's workspace (Eq. 1). Subsequently, the intersection point p_1 of the ray with the circle can be computed, enabling the straightforward derivation of angles θ_1 and θ_2 (Eq. 2).

$$y = s - (r_0 + \vec{r_d}((s - r_0) \cdot \vec{r_d})) \tag{1}$$

$$p_{1,\,2} = r_0 + \vec{r_d}(((s - r_0) \cdot \vec{r_d}) \pm \sqrt{r^2 - y^2}) \tag{2}$$

To make the operator's interaction with the robot more intuitive, the ray is controlled mainly through hand gestures and supported with voice commands to enable or disable different functions. Two interactive control methods were developed, denoted as gesture-based and auto-targeting.

For gesture-based targeting, the operator controls the robot's end-effector by initiating movement with a fist gesture and positioning the robot by manipulating the ray. Additionally, specific degrees of freedom (DoF) can be locked to facilitate minor adjustments along one dimension without

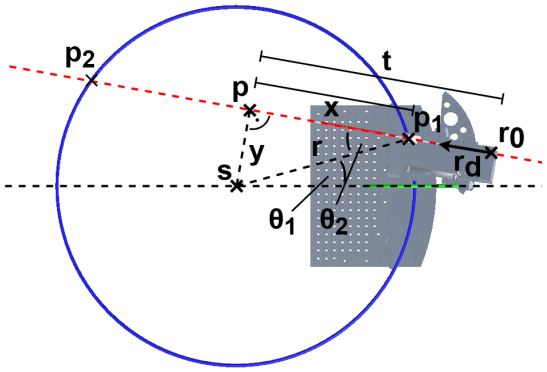

Fig. 5: The diagram visualizes the variables used in the IK calculations. The needle trajectory is depicted in red.

inadvertently impacting others. The surrogate robot will only start to move when the operator closes the right hand as a fist. Such a feature is common in commercial surgical robots, often activated by a foot pedal. The MRTK is employed to detect the operator's hands, from which gestures can be derived. Robot motion is defined by a proportional derivative (PD) controller that takes into account the error between the robot's end-effector and the ray, effectively filtering out high-frequency noise from the estimation of the hand position. To further enhance the stability of robot control, the hand's motion is down-scaled by a factor of 4, meaning that 100 mm of movement by the operator translates to 25 mm of movement of the robot. A beam is projected along the needle trajectory for easier pinpointing of targets with this method.

For auto-targeting, the operator can manipulate and move a holographic target to a desired position in the AR scene. Subsequently, the robot's end-effector will follow this movement, aligning the needle trajectory with the target. This target can be moved by the default interaction method built in the HMD (i.e. pinching gesture in Figure 6(b)). Besides that, different functions can be activated by voice commands or the graphical user interface (GUI, in Figure 1). The current joint positions are then sent as serial commands to the physical robot. Given that the robot uses pneumatic stepper motors, the joint positions must be converted to step positions of the motors. First, the change in angle per step is calculated, which depends on the gear ratio of the motor and the radius on which the joint moves. Equations 3 and 4 demonstrate the conversion from angle rate to step rate.

$$d_{\text{step13:10}} = 180/\pi \cdot 0.462/r_{\text{joint}} \tag{3}$$

$$d_{\text{step17:10}} = 180/\pi \cdot 0.604/r_{\text{joint}} \tag{4}$$

The workspace limits of the robot can then be calculated by equation 5.

$$p_{\text{min}} = \frac{\theta_{\text{min}}}{d_{\text{step}}}, p_{\text{max}} = \frac{\theta_{\text{max}}}{d_{\text{step}}} \tag{5}$$

Finally, the current joint angles are mapped to the step position with equation 6.

$$p_{\text{steps}} = p_{\text{min}} + (\frac{\theta - \theta_{\text{min}}}{\theta_{\text{max}} - \theta_{\text{min}}} \cdot (p_{\text{max}} - p_{\text{min}})) \tag{6}$$

The maximum displacement a step can empose on the needle tip is around 3 mm. As each plane is controlled by two stepper motors, this potential cause for inaccuracy is greatly reduced in practise.

D. Experimental evaluation

To benchmark the proposed method, a pseudo-randomized study involving ten subjects who have limited or no prior experience with AR was conducted. To evaluate the functional performance of the developed AR-based robot control, a bench-top study was designed to mimic the task loading of needle positioning and orientation in MR-guided breast biopsy. To simplify the procedure, the experiment only focused on the robot operation instead of medical imaging, so no MRI images were used. A sheet of paper containing ten designated targets was placed in a holder in front of the physical robot. In all cases, the physical robot was used to puncture the targets in the paper. Subjects were asked to reach the centre of each target on the paper by repositioning the needle of the Sunram 7 robot. Three different control methods were tested and subsequently compared in this manner. The first two methods correspond to those previously described (Section II-C): gesture-based control and auto-targeting mode. For AR-based methods, a corresponding 10 targets were also rendered in the AR scene with the same predetermined size and relative distance to the surrogate robot. By using the AR-based control methods to pinpoint the targets while the physical robot is coupled to the surrogates motion, the paper targets are punctured. The third method involved controlling the joint angles via three physical joysticks (shown in Figure 6(c)). Two of the joysticks control two DoFs each, moving the revolute joints, while the third one controls the prismatic joint, to which the needle is attached. The joystick sensitivity is fine enough to move singular steps of the stepper motors. For all three methods, the subjects committed to the targeting positions while the needle was fully retracted. Both the total time required to puncture all ten targets and the distance from the penetration point to the centre of each target were measured. The distance was measured with calipers. To minimize potential bias due to training effects, the order of the trials was adjusted for each subject. In the end, five subjects started with the AR-based methods followed by the joysticks, while the other five subjects started the other way around. Subsequently, the accuracy, precision, and task completion times were compared.

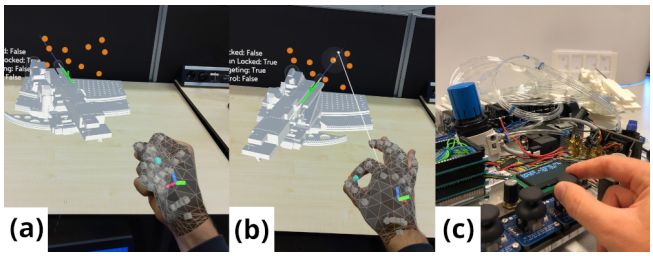

Fig. 6: The three different control methods from left to right: (a) Gesture control, (b) auto-targeting mode, and (c) joystick control.

III. RESULTS

Figure 7 provides an overview of all trials. It is noticeable that offsets from the centre of the target can be observed. Figure 8 displays the accuracy and precision of the incision point relative to the target center for all trials, along with the time spent on each trial. The leftmost comparison assesses the accuracy of the trials by analyzing the raw data collected (Figure 8(a)). The median accuracy was 2.24 for the gesture control method, 2.55 mm for the auto-targeting method, and 3.20 mm for the joystick control method. A pairwise analysis of variance (ANOVA) was conducted to identify significant differences between the methods. Both AR-based meth-

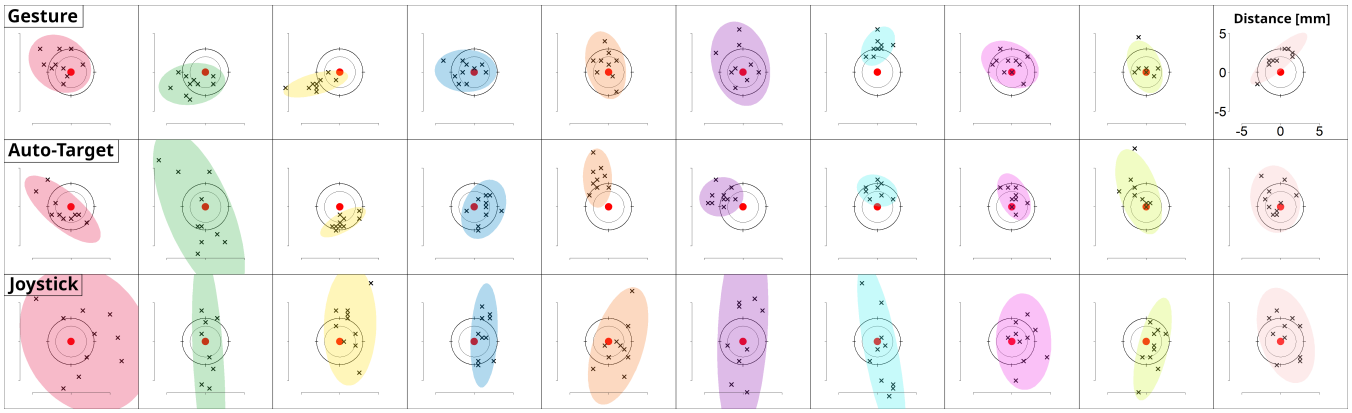

Fig. 7: The overview of all trials of ten subjects. The three rows represent the three different control methods used. The columns represent the different subjects. The radius of the outer circle in each target is 3mm.

ods showed significantly higher accuracy than the joystick method. To assess the precision of the methods, offsets (e.g. caused by calibration errors or subject-specific biases) were mitigated by subtracting the inter-subject mean vector from the trials. The resulting median scores were 1.50 mm, 1.50 mm, and 2.80 mm for gesture control, auto-targeting, and joystick control, respectively. The pairwise ANOVA revealed significant differences between the joystick control method and the AR-based methods, with the AR-based methods demonstrating significantly better performance. Finally, the time it took each subject to complete a trial (reach 10 targets) was assessed. On average, subjects took 279.1 $\pm$ 64.54 s for gesture control, 377 $\pm$ 83.42 s for auto-targeting, and 290.4 $\pm$ 70.59 s for joystick control to complete the trials. It shows significant differences between the auto-targeting method and the others, with the auto-targeting method performing significantly worse in terms of time efficiency.

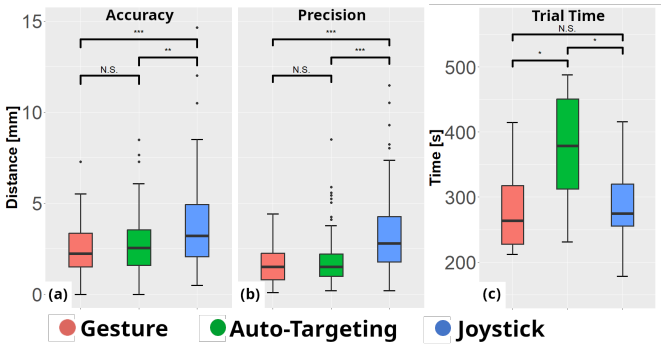

Fig. 8: Boxplots comparing the three different control methods. (a) Accuracy (b) Precision (c) The trial times for each of the methods in seconds. The lines above the plots indicate comparisons via a pairwise ANOVA. The three asterisks indicate statistical significance, while N.S. indicate no significance.

IV. DISCUSSION

In this paper, an AR-based control method in the medical field was developed to facilitate the procedure of MR-guided breast biopsy. A benchmark study was conducted, focusing on the evaluation of task loading of robotic breast biopsy, especially for biopsy needle positioning and orientation.

To facilitate this procedure, two interactive control methods were developed in AR, termed gesture-based control and auto-targeting. Both methods aimed to maximize the advantages of augmented reality as immersive interaction tools. The gesture-based control method couples the movement of the fist with the pose of the surrogates end-effector. By representing the physical robot with a digital surrogate, users can have an immersive control experience during the teleoperation of the biopsy needle. Real-time 3D holographic visualization in the AR scene also facilitates the visual perception of this biopsy procedure. The auto-targeting control method releases the control over the orientation from the user, by automatically aligning the needle trajectory with the target defined in the AR scene. This alleviates the clinicians from part of the targeting task, while leaving them in control over the robot position relative to the target, and subsequently the insertion point. Both AR interactive methods exhibited significant increases in accuracy and precision when compared to the joystick. While the subjects had visual feedback from the real targets on the paper when using the joystick control, they only had a virtual holographic representation of the targets with the AR-based methods. While it may not be a direct comparison between the joystick method and AR-based method, the authors would like to highlight that the main focus of this work is on task loading in the clinical setting for breast biopsy, with needle positioning and orientation as the primary tasks. In this context, this comparison is a reasonable study to investigate the potential of AR-based robot control methods for clinical applications in the future. Figure 7 reveals that many trials exhibited biases, which could have originated from various sources. With the joystick control method, there was a much greater spread of the distance to the target along the y-axis. This discrepancy could be attributed to the visual feedback being clearer in terms of the horizontal alignment of the biopsy needle to the target when sitting behind the robot. To mitigate these biases, the inter-subject mean vector was subtracted

from the trials, centring the average of each trial on the target. This allowed for the evaluation of the precision of the different methods. With the inter-subject mean subtracted, the median precision for both AR-based methods was almost twice as high as the joystick method. By only looking at the magnitude of the error, it seems to satisfy the requirements in biopsy as tumours smaller than 5 mm in diameter [17]. However, further investigations with experiments in a biopsy scenario must be conducted to draw such a conclusion in a clinical study. Compared with other's work, a targeting error of 4.4 $\pm$ 2.9 mm was reported as a good result of the real biopsy scenario [18]. These results demonstrate that the proposed methods, especially with the potential for further precision improvement, effectively address the concern expressed in other literature that AR might be too sensitive for precise control [11] by implementing PD control and gesture motion down-scaling. The AR-based methods showed no advantage in trial time, while the auto-targeting method even experienced a worse outcome. That being said, in practise, the operator will only have to pinpoint one target during the procedure, which makes the targeting time less significant in relation to the whole procedure. Even though the auto-targeting method allows the robot to automatically track a predefined target and the user to give fewer inputs, it became the longest procedure in general. This indicates that this approach proved to be challenging for the subjects to adapt to, which represented the most significant limitation of the auto-targeting method.

In this work, we only evaluated the system under bench-top experiments specializing in needle positioning and orientation procedures. To improve the system further, a clinical study shall be planned in the future to test the feasibility of the developed system under conditions of a real MRI procedure. To do so, future work includes MRI imaging integration with an image-based feedback loop for the optimization of needle injection. This will involve representing the patient's anatomical structures along with the target lesion as a hologram directly constructed from MRI images.

V. CONCLUSIONS

An AR-based digital twin control scheme to interact with an MR safe robot has been developed. This scheme involves creating a virtual surrogate of the physical robot, enabling intuitive interaction to adjust the pose of the biopsy needle. The results showed the good potential of utilizing such a virtual surrogate robot as the digital twin of the physical one to execute a dedicated task, like needle steering and injection. In the future, it is essential to integrate the system into a real MR environment to close the loop between the imaging process and the biopsy procedure. This integration would potentially pave a new way of interacting with medical robots for clinical applications requiring teleoperation.

REFERENCES

[1] Siegel RL, Miller KD, Fuchs HE, Jemal A. Cancer statistics, 2022. CA Cancer J Clin. 2022 Jan;72(1):7-33. doi: 10.3322/caac.21708. Epub 2022 Jan 12. PMID: 35020204.

[2] Kuhl, C., Schrading, S., Leutner, C., Morakkabati-Spitz, N., Wardelmann, E., Fimmers, R., Kuhn, W., Schild, H. (2005). Mammography, Breast Ultrasound, and Magnetic Resonance Imaging for Surveillance of Women at High Familial Risk for Breast Cancer. Journal of clinical oncology : official journal of the American Society of Clinical Oncology. 23. 8469-76. 10.1200/JCO.2004.00.4960.

[3] Papalouka V, Kilburn-Toppin F, Gaskarth M, Gilbert F. MRI-guided breast biopsy: a review of technique, indications, and radiological-pathological correlations. Clin Radiol. 2018 Oct;73(10):908.e17-908.e25. doi: 10.1016/j.crad.2018.05.029. Epub 2018 Jul 2. PMID: 30041954.

[4] H. Ranjan, M. van Hilten, V. Groenhuis, J. Verde, A. Garcia, S. Perretta, J. Veltman, F.J. Siepel, S. Stramigioli, "Sunram 7: An MR Safe Robotic System for Breast Biopsy". IEEE/RSJ International Conference on Intelligent Robots and Systems (IROS), Oct 2023, pp. In press.

[5] Morales Mojica CM, Velazco-Garcia JD, Pappas EP, Birbilis TA, Becker A, Leiss EL, Webb A, Seimenis I, Tsekos NV. A Holographic Augmented Reality Interface for Visualizing of MRI Data and Planning of Neurosurgical Procedures. J Digit Imaging. 2021 Aug;34(4):1014-1025. doi: 10.1007/s10278-020-00412-3. Epub 2021 May 23. PMID: 34027587; PMCID: PMC8455790.

[6] Ryo Suzuki, Adnan Karim, Tian Xia, Hooman Hedayati, and Nicolai Marquardt. 2022. Augmented Reality and Robotics: A Survey and Taxonomy for AR-enhanced Human-Robot Interaction and Robotic Interfaces. In Proceedings of the 2022 CHI Conference on Human Factors in Computing Systems (CHI '22). Association for Computing Machinery, New York, NY, USA, Article 553, 1–33.

[7] Vörös, Viktor, Li, Ruixuan, Davoodi, Ayoob, Wybaillie, Gauthier, Vander Poorten, Emmanuel and Niu, Kenan. (2022). An Augmented Reality-Based Interaction Scheme for Robotic Pedicle Screw Placement. Journal of Imaging. 8. 273. 10.3390/jimaging8100273.

[8] Feig S. Cost-effectiveness of mammography, MRI, and ultrasonography for breast cancer screening. Radiol Clin North Am. 2010 Sep;48(5):879-91. PMID: 20868891.

[9] Z. Lin et al., "ARei: Augmented-Reality-Assisted Touchless Teleoperated Robot for Endoluminal Intervention," in IEEE/ASME Transactions on Mechatronics, vol. 27, no. 5, pp. 3144-3154, Oct. 2022.

[10] C. M. Morales Mojica et al., "Interactive and Immersive Image-Guided Control of Interventional Manipulators with a Prototype Holographic Interface," 2019 IEEE 19th International Conference on Bioinformatics and Bioengineering (BIBE), Athens, Greece, 2019, pp. 1002-1005.

[11] J. D. Velazco-Garcia et al., "Evaluation of how users interface with holographic augmented reality surgical scenes: Interactive planning MR-Guided prostate biopsies," The International Journal of Medical Robotics and Computer Assisted Surgery, vol. 17, no. 5. Wiley, Jun. 08, 2021.

[12] C. Xue, Y. Qiao and N. Murray, "Enabling Human-Robot-Interaction for Remote Robotic Operation via Augmented Reality," 2020 IEEE 21st International Symposium on "A World of Wireless, Mobile and Multimedia Networks" (WoWMoM), Cork, Ireland, 2020, pp. 194-196.

[13] A. Aristidou and J. Lasenby, "FABRIK: A fast iterative solver for the Inverse Kinematics problem", Graphical Models, vol. 73, no. 5, 2011, pp. 243-260

[14] C. P. Quintero, S. Li, M. K. Pan, W. P. Chan, H. F. Machiel Van der Loos and E. Croft, "Robot Programming Through Augmented Trajectories in Augmented Reality," 2018 IEEE/RSJ International Conference on Intelligent Robots and Systems (IROS), Madrid, Spain, 2018, pp. 1838-1844.

[15] M. E. Walker, H. Hedayati and D. Szafir, "Robot Teleoperation with Augmented Reality Virtual Surrogates," 2019 14th ACM/IEEE International Conference on Human-Robot Interaction (HRI), Daegu, Korea (South), 2019, pp. 202-210.

[16] V. Groenhuis and S. Stramigioli, "Rapid Prototyping High-Performance MR Safe Pneumatic Stepper Motors," in IEEE/ASME Transactions on Mechatronics, vol. 23, no. 4, pp. 1843-1853, Aug. 2018.

[17] Raza S, Sekar M, Ong EM, Birdwell RL. Small masses on breast MR: is biopsy necessary? Acad Radiol. 2012 Apr;19(4):412-9. Epub 2012 Jan 24. PMID: 22277636.

[18] El Khouli RH, Macura KJ, Barker PB, Elkady LM, Jacobs MA, Vogel-Claussen J, Bluemke DA. MRI-guided vacuum-assisted breast biopsy: a phantom and patient evaluation of targeting accuracy. J Magn Reson Imaging. 2009 Aug;30(2):424-9. PMCID: PMC2735014.